forests

MDPI

Article

Similar Pattern of Potential Distribution of *Pinus yunnanensis* Franch and *Tomicus yunnanensis* Kirkendall under Climate Change in China

Biaosheng Huang [1], Jiawei Mao [1], Youjie Zhao [1,*], Yongke Sun [1], Yong Cao [1] and Zhi Xiong [2]

[1] College of Big Data and Intelligent Engineering, Southwest Forestry University, Kunming 650224, China
[2] College of Further Education, Southwest Forestry University, Kunming 650224, China
* Correspondence: bioala@swfu.edu.cn

Abstract: *Tomicus yunnanensis* Kirkendall (Coleoptera: Scolytinae) is a stem-boring pest that endangers *Pinus yunnanensis* Franch (Pinales:Pinoideae), which seriously affects the ecological environment safety in southwest China. In order to understand the potential distribution pattern and change in the potential distribution of *P. yunnanensis* and *T. yunnanensis*, this study used the maximum entropy model to predict the distribution of potentially suitable areas for *P. yunnanensis* and *T. yunnanensis* and explored the relationships between their different spatiotemporal distributions based on change analysis. The experimental results show that altitude is the main factor restricting the current distribution of *P. yunnanensis*. The current suitable areas of *P. yunnanensis* are mainly distributed in Yunnan, Sichuan and Guizhou. The minimum temperature of the coldest month is the main factor affecting the current distribution of *T. yunnanensis*. The current suitable areas of *T. yunnanensis* are mainly distributed in Yunnan, Sichuan and Tibet. Under future climate scenarios, the total suitable areas of *P. yunnanensis* and *T. yunnanensis* are expected to increase. The suitable areas tend to move to higher altitudes in the west and higher latitudes in the north. At the same time, this study finds that there is an obvious bottleneck of expansion to northeastern Sichuan near the Daba Mountains. The results of intersection analysis showed that, with future climate change, *P. yunnanensis* and *T. yunnanensis* mainly showed lowly suitable (or unsuitable)—lowly suitable (or unsuitable) to moderately (or highly) suitable—and moderate (or high) variation patterns of suitable areas under the SSP1-2.6 climate scenario. These results will provide an important basis for the breeding of *P. yunnanensis* and controlling *T. yunnanensis*.

Keywords: *Pinus yunnanensis*; *Tomicus yunnanensis*; maximum entropy model; environmental variables; potential distribution; suitable areas

check for updates

Citation: Huang, B.; Mao, J.; Zhao, Y.; Sun, Y.; Cao, Y.; Xiong, Z. Similar Pattern of Potential Distribution of *Pinus yunnanensis* Franch and *Tomicus yunnanensis* Kirkendall under Climate Change in China. *Forests* **2022**, *13*, 1379. https://doi.org/10.3390/f13091379

Academic Editors: Nadezhda Tchebakova and Sergey V. Verkhovets

Received: 22 July 2022
Accepted: 26 August 2022
Published: 29 August 2022

Publisher's Note: MDPI stays neutral with regard to jurisdictional claims in published maps and institutional affiliations.

Copyright: © 2022 by the authors. Licensee MDPI, Basel, Switzerland. This article is an open access article distributed under the terms and conditions of the Creative Commons Attribution (CC BY) license (https://creativecommons.org/licenses/by/4.0/).

1. Introduction

Global climate change has seriously affected forests with different biomes and ecosystems' stability, which is one of the crucial factors that affect the distribution of species and causes huge economic losses. According to the Sixth Assessment Report (AR6) "Climate Change 2021: The Physical Science Basis", released by the Intergovernmental Panel on Climate Change (IPCC) in August 2021, global warming is expected to continue, with the average Earth's surface temperature rising by 0.3–4.5 degrees Celsius by 2100 compared to 1986 to 2005 [1]. According to the Blue Book of China Climate Change (2021), released by the Climate Change Center of the China Meteorological Administration, China is a sensitive and significant area of global climate change, and its temperature rise rate is significantly higher than the global average level in the same period. From 1951–2020, China's annual mean surface temperature has shown a significant upward trend with a rate of 0.26 °C/decade, and the average precipitation has shown an upward trend [2,3]. Previous studies showed [4–6] that global climate change, especially the rise of average temperature, posed a serious threat to the sustainability of the global ecosystem and hugely

impacted species distribution. The synergistic effect of global climate change, human activities and biological invasions may lead to habitat destruction and increase the risk of species extinction [7]. Land-use changes caused by human activities, such as changes in management practices and land use, lead to habitat fragmentation, which has exerted great impacts on species distribution and climate change in China [8,9]. Balint et al. [10] pointed out that climate change is an important driver of biodiversity loss, habitat fragmentation and species spatial pattern changes. Therefore, understanding species distribution dynamics under climate change is crucial for making conservation plans and assessing the potential impacts of climate change on species migration [11].

Species distribution and richness are important indicators to protect biological diversity under global climate change [12]. Currently, species distribution models (SDMs) have been widely used in studies of species distribution on the impact of climate change, mainly to evaluate species occurrence or richness and spatial distribution [13,14]. SDMs are based on species' known distribution points and environmental factors, using a mathematical algorithm to construct models, determine the distribution of the species unknown probability and then estimate its distribution in the whole ecological niche space, finally through the distribution of mapping to the study of geographic space for the regional distribution of species of potential [8,15]. At present, commonly used SDMs mainly include the Bioclimate Analysis and Prediction System (BIOCLIM), Ecological Niche Factor Analysis (ENFA), Genetic Algorithm for rule-set Production (GARP) and Maximum Entropy Modeling (MaxEnt) [15]. However, SDMs only consider environmental factors affecting species distribution and lack analysis of interactions between species and prediction of the potential distribution of species [16]. Currently, the MaxEnt model is a commonly used prediction model for species-suitable areas and can obtain good prediction results with few species distribution points. At the same time, the MaxEnt model is simple to operate and has been proven to be the most reliable SDM model [5]. The MaxEnt model has been widely used in agriculture [17–20], forestry [21,22], fisheries [23–26], endangered animal and plant protection [27–30] and pest prediction and control [31–34].

There are more than 113 formally recognized species of the genus *Pinus*, mainly distributed in the northern hemisphere; they form an important part of forest ecosystems [35]. *Pinus yunnanensis* Franch is mainly distributed in Yunnan, Sichuan, Guizhou, Guangxi and Tibet. It is a major timber and afforestation tree species in Yunnan Province, with an area of more than 4.8 million hm^2 [36]. *Tomicus yunnanensis* Kirkendall and Faccoli is a stem-boring pest that harms a variety of pine plants. It is only distributed in Yunnan Province, Guizhou Province, Sichuan Province and other regions of China [37]. It is one of the main pests of *P. yunnanensis*. It occurs on a large scale every year and continues to spread to Sichuan Province, Guizhou Province and other places, seriously affecting the ecological and environmental security in southwest China [38]. However, there are few studies on the potential distribution relationship between *P. yunnanensis* and *T. yunnanensis* under climate change.

Based on the current distribution data of *P. yunnanensis* and *T. yunnanensis*, this study intends to use the MaxEnt model to predict the distribution of *P. yunnanensis* and *T. yunnanensis* and comparative analysis of suitability classes of potentially suitable areas based on factors such as future climatic conditions, topography and soil. The main contributions of this study are: (1) revealing the dominant environmental factors affecting the growth of *P. yunnanensis* and *T. yunnanensis*, (2) modeling the potential adaptation of *P. yunnanensis* and *T. yunnanensis* under current and future climate scenarios and (3) exploring the relationship between *P. yunnanensis* and *T. yunnanensis*, which provides resources for the breeding and cultivation of *P. yunnanensis* and the control of *T. yunnanensis*.

2. Materials and Methods

2.1. Species Occurrence Data and Environmental Factors

The distribution data of *P. yunnanensis* and *T. yunnanensis* were mainly collected through the Global Biodiversity Information Facility (https://www.gbif.org/zh/ accessed on 8 June 2022),

the National Herbarium Teaching Specimen Resource Sharing Sub-Bank (http://mnh.scu.edu.cn/ accessed on 8 June 2022) and the China Journal Full-text Database (https://www.cnki.net/ accessed on 8 June 2022). After the data were acquired, the latitude and longitude were uniformly converted into a decimal by using the latitude and longitude conversion formula to realize the distribution data and the basic geospatial data. To prevent density distribution between *P. yunnanensis* and *T. yunnanensis*, dense distribution points would cause problems, such as the overfitting of the model. In this study, the duplicated data were first removed, and only one record was kept. Second, the distribution data of *P. yunnanensis* and *T. yunnanensis* were loaded into ArcGIS (version 10.8) to check for correct identification, and the Spatially Rarefy Occurrence Data for SDMs in the SDM Toolbox was used according to the principle that the distance between *P. yunnanensis* and *T. yunnanensis* was greater than 50 m. A total of 74 distribution points of *P. yunnanensis* and 14 distribution points of *T. yunnanensis* were finally selected. After the data processing, the distribution data were saved as a CSV file according to the species name, longitude and latitude.

A total of 24 environmental factors in 3 categories that influence the growth of *P. yunnanensis* and *T. yunnanensis* were selected for subsequent analysis (Table 1). The climate factors were obtained from the World Climate Database (https://www.worldclim.org/ accessed on 9 June 2022) with a spatial resolution of 2.5 min. The current climate factors used in this study were 19 bioclimatic factors (BIO1-BIO19) from 1970–2000 and elevation variables (ELEV). The soil and vegetation factors came from the National Qinghai–Tibet Plateau Data Science Center (http://data.tpdc.ac.cn/zh-hans/ accessed on 9 June 2022). Soil factors mainly include soil available water content (AWC_CLASS), soil pH (T_PH_H_2O) and carbonate or lime content (T_$CACO_3$), and vegetation factors mainly include vegetation type (VEGETATION). Due to the lack of future topographic data on climate change, this study defaults that the national topography will not change during the forecast period [4]. The base map of China came from the National Basic Geographic Information System (http://nfgis.nsdi.gov.cn/ accessed on 9 June 2022).

Table 1. The 24 environmental factors used in this study.

Type	Environmental Factors	Description of Environmental Factors
Temperature	BIO1	Annual Mean Temperature
	BIO2	Mean Diurnal Range
	BIO3 *	Isothermality
	BIO4	Temperature Seasonality
	BIO5	Maximum Temperature of Warmest Month
	BIO6 *	Minimum Temperature of Coldest month
	BIO7 *	Temperature Annual Range
	BIO8	Mean Temperature of Wettest Quarter
	BIO9	Mean Temperature of Driest Quarter
	BIO10	Mean Temperature of Warmest Quarter
	BIO11	Mean Temperature of Coldest Quarter
Precipitation	BIO12	Annual Precipitation
	BIO13	Precipitation of Wettest Month
	BIO14	Precipitation of Driest Month
	BIO15 *	Precipitation Seasonality
	BIO16	Precipitation of Wettest Quarter
	BIO17	Precipitation of Driest Quarter
	BIO18	Precipitation of Warmest Quarter
	BIO19 *	Precipitation of Coldest Quarter
Terrain	ELEV *	Elevation

Table 1. *Cont.*

Type	Environmental Factors	Description of Environmental Factors
Soil	AWC_CLASS *	Soil's available water content
	T_CACO3 *	Soil's carbonate or lime content
	T_PH_H2O *	Soil's pH
Vegetation	VEGETATION *	Vegetation type

* Indicates the environmental factors involved in MaxEnt modeling after filtering.

The future environmental factor variables in this study were selected from the BCC-CSM2-MR model in the World Climate Database. The emission paths were the future climate scenarios of SSP1-2.6 and SSP5-8.5 of shared social economy pathways (SSPs). The BCC-CSM2-MR model came from the Sixth International Coupling Model Comparison Program (CMIP6), which was a climate system model developed by the Beijing Climate Center. It accurately predicts variables such as temperature and precipitation [39]. Future climate forecasts include two periods, 2021–2040 and 2061–2080. All environmental factor variables were converted to ASCII format for MaxEnt analysis.

2.2. Environmental Factor Pre-Process

Previous studies have revealed the problem of multicollinearity among variables of environmental factors [21,40,41]. In order to avoid excessive fitting of the model and multiple linear relationships among variables, environmental factors were pretreated in this study. First, the environmental factors with similar properties were removed. Secondly, the Remove Highly Correlated Variables tool in the SDM Toolbox of ArcGIS was used to calculate the correlation among 24 environmental factor variables (Figure 1). If there were two or more environmental factor correlation coefficients $|r| \geq 0.8$, the variable with the clearer ecological significance was retained. The filtered factors are shown in Table 1.

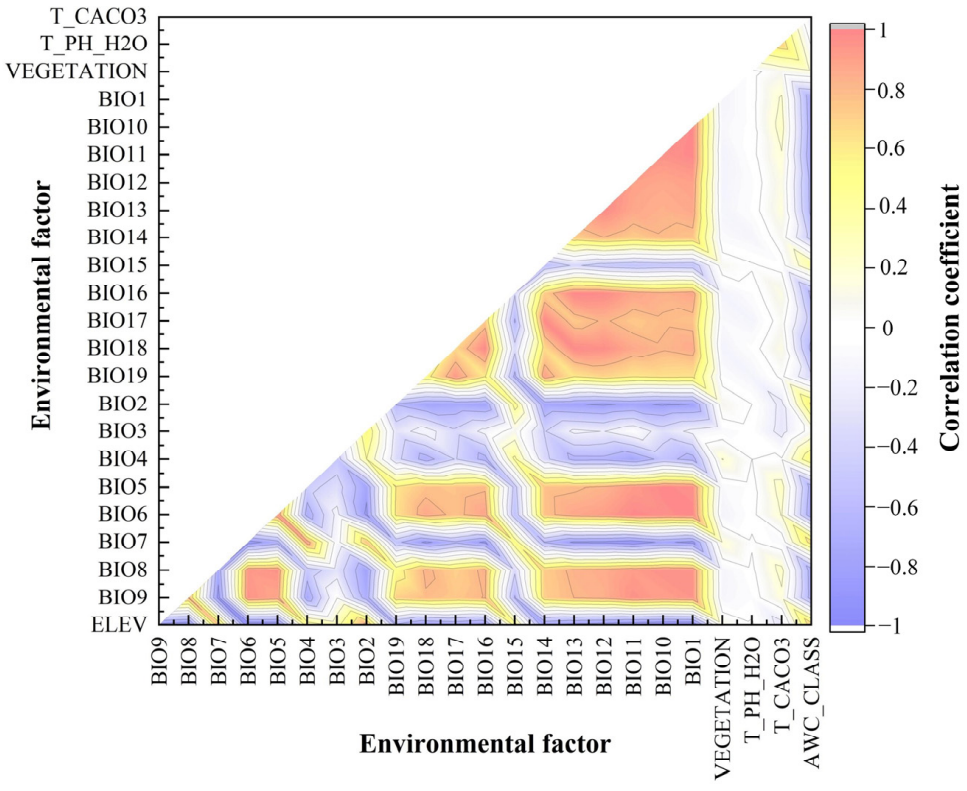

Figure 1. Matrix of environmental factor correlation coefficients.

2.3. MaxEnt Model Construction and Result Evaluation

Based on the processed samples of *P. yunnanensis* and *T. yunnanensis*, the selected environmental factors were input into the MaxEnt model, 75% of the data were randomly selected as the training set for model construction, and the remaining 25% were used as the test set for model evaluation. The model was iterated 10 times, "Bootstrap" was selected for the iteration run type, and the default parameters were used for the others. For potential distribution predictions under future climates, future environmental factor variables need to be entered into the projection layers directory/file column, and 10 iterations were used to average each run.

In this study, the nonparametric estimation of the Jackknife method was used to evaluate the contribution rate of each environmental factor and the receiver operating characteristic (ROC) curve of the influence of each environmental variable on the distribution of *P. yunnanensis* and *T. yunnanensis*. The area under the ROC curve (AUC) was used to evaluate the accuracy of model predictions [40,41]. AUC values range from [0.5, 1], and typically, model performance was classified as failing (0.5–0.6), poor (0.6–0.7), fair (0.7–0.8), good (0.8–0.9) or excellent (0.9–1.0). AUC values close to 1 indicated that the model predicts more accurate results [42]. The relative contribution of each environmental factor to the model was evaluated according to the percentage contribution rate of environmental factors output by the MaxEnt model. The dominant environmental factors affected the geographical distribution of *P. yunnanensis* and *T. yunnanensis*.

The MaxEnt model estimated the suitable probability (P) of species in each grid in ASCII format, and the value range is [0,1]. First, the *.asc format was converted to raster format by using the conversion tool in ArcGIS. Then the reclassification tool in the analysis tool was used to divide the fitness level, and the maximum training sensitivity and specificity (MaxSS) [43] method was used to determine the threshold (y); when the existence probability of a species in a certain area P < y, it is defined as an unsuitable area. Then the mean value of (1-y) was used to define the lowly suitable areas, the moderately suitable areas and the highly suitable areas. Finally, the reclassification results are saved in raster format. The habitat suitability of *P. yunnanensis* was divided into unsuitable areas (0–0.2833), lowly suitable areas (0.2833–0.5222), moderately suitable areas (0.5222–0.7611) and highly suitable areas (0.7611–1) according to the definition of suitability grades from low to high. The habitat suitability of *T. yunnanensis* was divided into unsuitable areas (0–0.2423), lowly suitable areas (0.2423–0.4949), moderately suitable areas (0.4949–0.7475) and highly suitable areas (0.7475–1). Then this study calculated suitable areas under different climate scenarios by using calculated geometry.

2.4. Changes in the Potential Distribution of P. yunnanensis and T. yunnanensis

According to current and two different future climate change scenarios, the geographical distribution maps for current, 2021–2040 and 2061–2080 were created, and the potential distribution maps of *P. yunnanensis* and *T. yunnanensis* were compared. With a view to determine the spatial changes in the distribution, the data from different time periods in the raster format were converted into vectors using the raster–vector conversion tool in ArcGIS (Version10.8, Environmental Systems Research Institute Inc., Redlands, CA, USA). Intersection analysis was performed on the vector data to compute and analyze the differences [20,28].

3. Results

3.1. Model Accuracy Evaluation

The ROC curve was used to test the accuracy of the prediction of suitable areas for *P. yunnanensis* and *T. yunnanensis*. The average training AUC of the model, as shown in Figure 2, and the average AUC values are all over 0.9, which indicates that the model has excellent accuracy. Therefore, the MaxEnt (MaxEnt.jar) model can accurately simulate the potential geographic distribution of *P. yunnanensis* and *T. yunnanensis*.

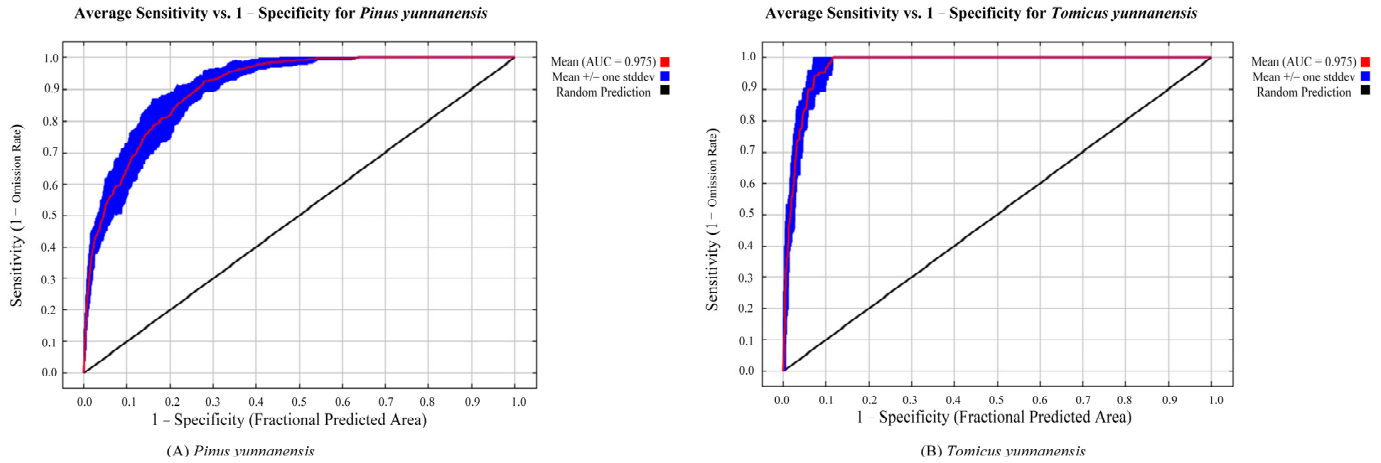

Figure 2. ROC curves and mean test AUC (10 replicate runs) of (**A**) *P. yunnanensis* and (**B**) *T. yunnanensis*.

3.2. Environmental Factors Affecting the Distribution of P. yunnanensis and T. yunnanensis

Figure 3 shows the percentage contribution of each environmental factor output from the MaxEnt model to predict the current of *P. yunnanensis* and *T. yunnanensis*. The realization results show that under the current climate environment, altitude (43.6%), isothermality (14.1%), the minimum temperature of the coldest month (9.3%), soil's available water content (8.9%), annual temperature range (7.8%) and topsoil carbonate or lime content (7.5%) are the dominant environmental factors affecting the potential distribution of *P. yunnanensis*. The soil's available water content (31.6%), isothermality (29.7%) and the minimum temperature of the coldest month (29.2%) are the dominant environmental factors that affect the potential distribution of *T. yunnanensis*. Under the future climate scenario model, the dominant environmental factors affecting the potential distribution of *P. yunnanensis* and *T. yunnanensis* are the same as those under the current climate environment.

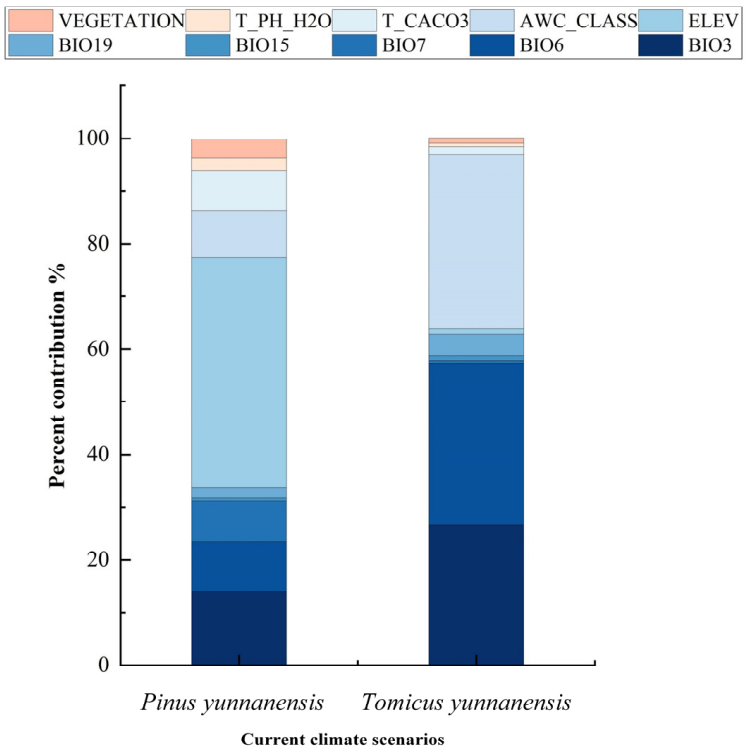

Figure 3. Percentage of environmental factors of *P. yunnanensis* and *T. yunnanensis*.

Using the Jackknife method to evaluate the impact of various environmental factors on predicting the current (Figure 4), the experimental results show that among the environmental factors affecting the potential distribution of *P. yunnanensis*, the single variable of elevation (ELEV) has the largest gain in modeling which indicates that this variable carries the most valuable information for modeling. The minimum temperature of the coldest month (BIO6) and annual temperature range (BIO7) also contribute significantly to the modeling. Among the environmental factors that affect the potential distribution of *T. yunnanensis*, the minimum temperature of the coldest month (BIO6) has the largest gain in modeling. When it is excluded alone, the gain decreases the most, which indicates that this variable carries the necessary modeling requirements and has the most valuable information.

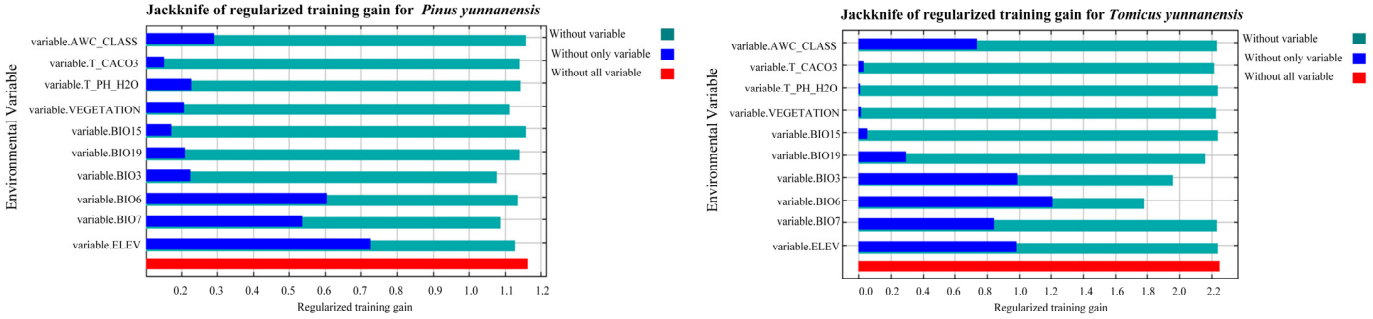

(A) *Pinus yunnanensis* (B) *Tomicus yunnanensis*

Figure 4. Jackknife test of variable importance in the species ((**A**) *P. yunnanensis*; (**B**) *T. yunnanensis*).

3.3. The Current Potential Distribution of P. yunnanensis and T. yunnanensis

The MaxEnt model was used to predict the current potential distribution of *P. yunnanensis* and *T. yunnanensis* (Figure 5, Table 2). The highly suitable areas of *P. yunnanensis* are scattered, while those of *T. yunnanensis* are more concentrated. The area of the highly suitable areas of *P. yunnanensis* is about 5.92 × 104 km^2, and the area of the moderately suitable areas is about 24.09 × 10^4 km^2. The area of the highly suitable areas of *T. yunnanensis* is about 4.31 × 10^4 km^2, and the area of the moderately suitable areas is about 9.14 × 10^4 km^2.

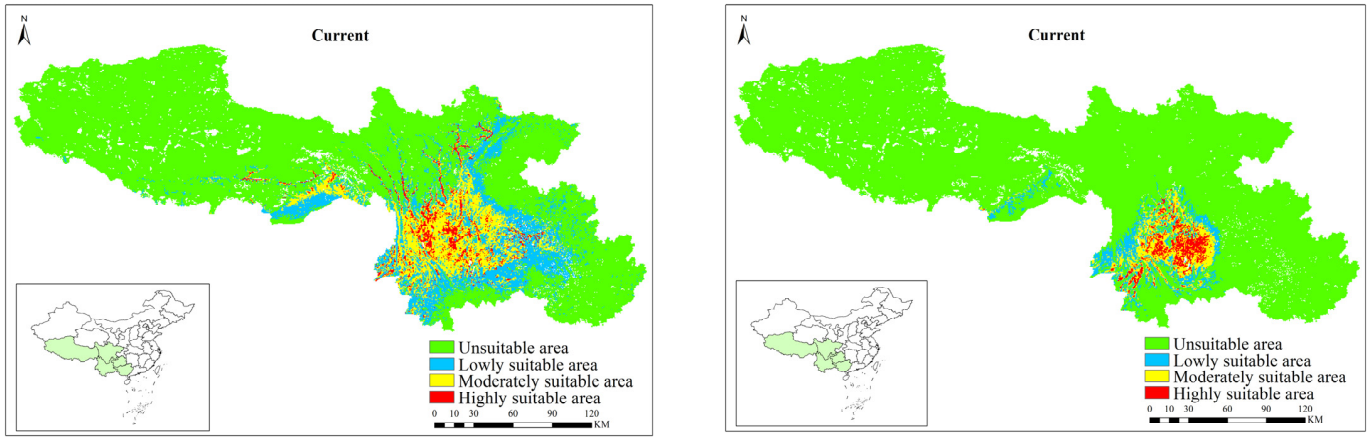

(A) *Pinus yunnanensis* (B) *Tomicus yunnanensis*

Figure 5. Potential distribution of (**A**) *P. yunnanensis* and (**B**) *T. yunnanensis* under current climatic conditions.

Table 2. Predicted suitable areas of *P. yunnanensis* and *T. yunnanensis* under different climate scenarios.

Species	Climate Scenarios		Total Suitable Area		Lowly Suitable Area		Moderately Suitable Area		Highly Suitable Area	
			Area ($\times 10^4$ km^2)	Trend (%)	Area ($\times 10^4$ km^2)	Trend (%)	Area ($\times 10^4$ km^2)	Trend (%)	Area ($\times 10^4$ km^2)	Trend (%)
P. yunnanensis	Current	1970–2000	63.42		33.40		24.09		5.92	
	SSP1-2.6	2021–2040	111.12	75.21	47.97	43.62	63.08	161.85	0.08	−98.64
		2061–2080	111.72	76.15	22.43	−32.84	81.43	238.02	7.86	32.77
	SSP5-8.5	2021–2040	111.28	75.47	21.67	−35.11	81.32	237.67	8.29	40.03
		2061–2080	90.78	43.14	75.62	126.40	13.03	−45.91	1.86	−68.58
T. yunnanensis	Current	1970–2000	22.81		9.36		9.14		4.31	
	SSP1-2.6	2021–2040	54.78	140.15	14.15	51.12	18.25	99.67	22.38	419.26
		2061–2080	59.47	160.71	17.07	82.31	19.04	108.32	23.35	441.76
	SSP5-8.5	2021–2040	53.94	136.48	19.63	109.72	15.73	72.10	18.57	330.85
		2061–2080	35.12	53.97	11.68	24.79	11.65	27.46	12.18	182.60

Trend (%) reflects the percentage of area change compared to the current climate.

3.4. The Future Potential Distribution of *P. yunnanensis* and *T. yunnanensis*

This study analyzed the potential distribution of *P. yunnanensis* and *T. yunnanensis* under two shared socioeconomic pathways (SSP1-2.6 and SSP5-8.5) during two future periods (2021–2040 and 2061–2080) (Figures 6 and 7, Table 2). Under the future climate scenario, the suitable areas of *P. yunnanensis* and *T. yunnanensis* will increase and expand to the northeast. Under the SSP1-2.6 climate scenario, the area of suitable areas for *P. yunnanensis* and *T. yunnanensis* shows an overall upward trend. At the same time, there is an overall upward and then a downward trend under the SSP2-8.5 climate scenario.

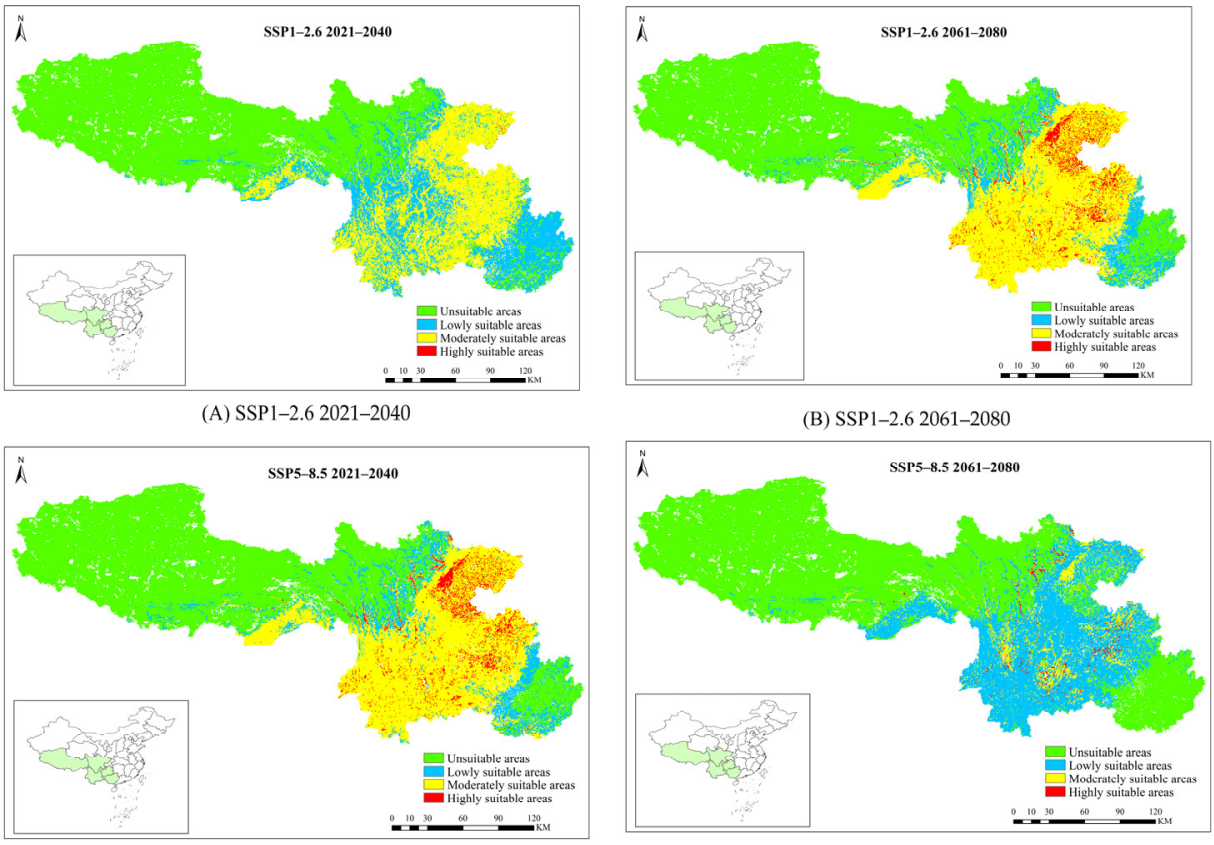

(A) SSP1–2.6 2021–2040 (B) SSP1–2.6 2061–2080

(C) SSP5–8.5 2021–2040 (D) SSP5–8.5 2061–2080

Figure 6. The future potential distribution of *P. yunnanensis* under different climate scenarios.

Under the SSP1-2.6 climate scenario, the area of lowly suitable areas for *P. yunnanensis* from 2021 to 2040 is expected to increase in southeastern Tibet, western Yunnan and eastern

Guangxi. The area of moderately suitable areas is expected to increase in northeastern Sichuan, Guizhou and southeastern Yunnan, while the highly suitable areas will be mostly reduced. Compared with 2021–2040, the area of the lowly suitable area of *P. yunnanensis* shrinks by half from 2061 to 2080, while the moderately suitable areas increase by about 18.35×10^4 km^2, which are mainly distributed in southeastern Tibet, Yunnan, Guizhou, eastern Sichuan and Western Guangxi. The highly suitable areas of *P. yunnanensis* increase by about 7.78×10^4 km^2, mainly distributed in eastern Sichuan and western Guizhou. Under the SSP5-8.5 climate scenario, the area of the moderately suitable areas of *P. yunnanensis* shrink slightly from 2021 to 2040 and the area of the moderately suitable areas is expected to increase in southeastern Tibet, Yunnan, Guizhou, eastern Sichuan and western Guangxi, while the area of highly suitable areas is expected to increase in eastern Sichuan and western Guizhou. From 2061 to 2080, the total area of the suitable growth areas of *P. yunnanensis* will shrink. Compared with 2021 to 2040, the lowly suitable areas will increase by about 53.95×10^4 km^2, while the moderately suitable areas will shrink significantly by about 68.29×10^4 km^2, and the area of the highly suitable areas will shrink by about 6.43×10^4 km^2.

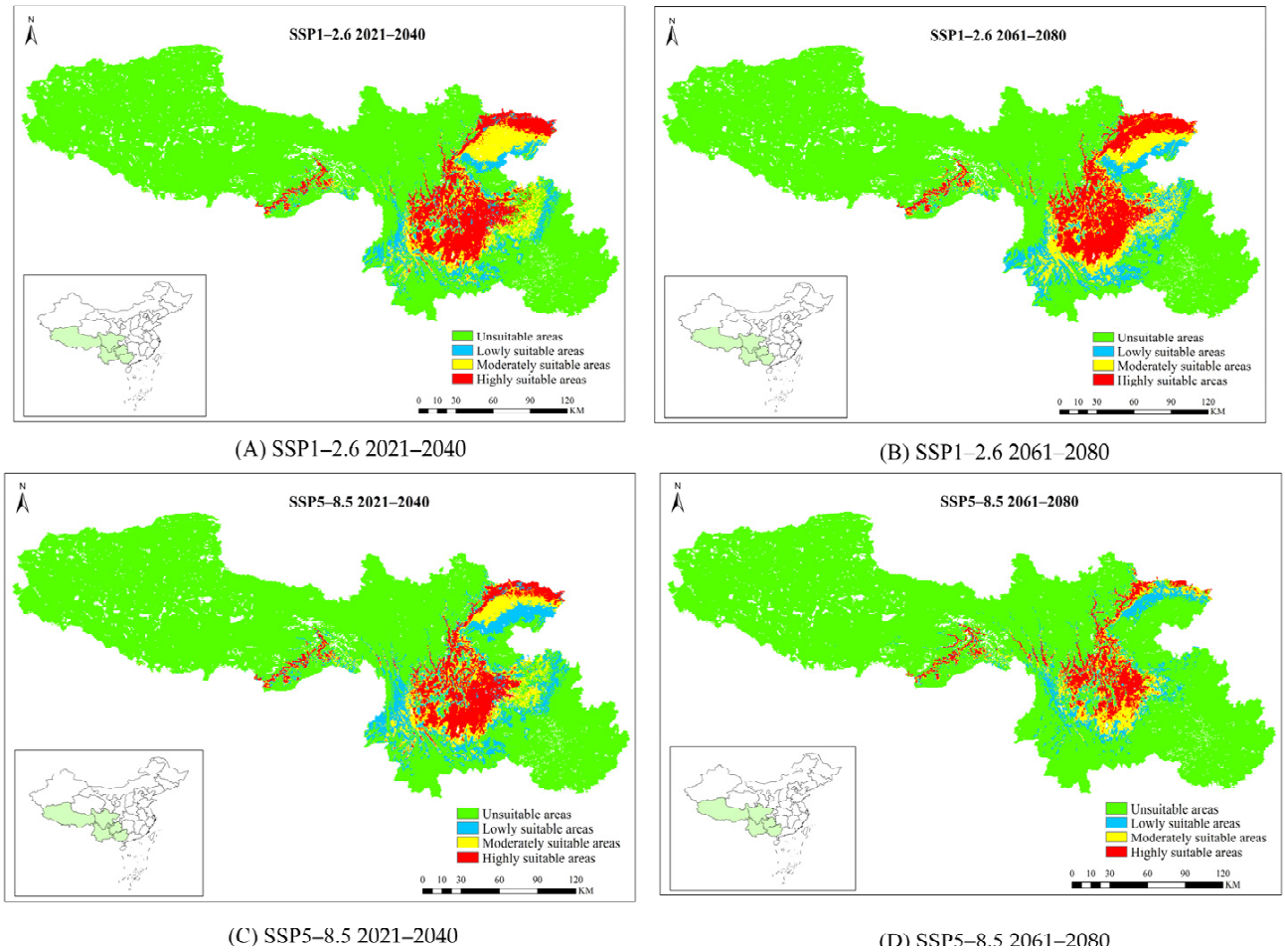

(A) SSP1–2.6 2021–2040 (B) SSP1–2.6 2061–2080

(C) SSP5–8.5 2021–2040 (D) SSP5–8.5 2061–2080

Figure 7. The future potential distribution of *T. yunnanensis* under different climate scenarios.

Under the SSP1-2.6 climate scenario, the area of lowly suitable areas for *P. yunnanensis* from 2021 to 2040 is expected to increase in southeastern Tibet, western Yunnan and eastern Guangxi. The area of moderately suitable areas is expected to increase in northeastern Sichuan, Guizhou and southeastern Yunnan, while the highly suitable areas will be mostly reduced. Compared with 2021–2040, the area of the lowly suitable area of *P. yunnanensis* shrinks by half from 2061 to 2080, while the moderately suitable areas increase by about 18.35×10^4 km^2, which are mainly distributed in southeastern Tibet, Yunnan, Guizhou,

eastern Sichuan and Western Guangxi. The highly suitable areas of *P. yunnanensis* increase by about 7.78 × 10^4 km^2, mainly distributed in eastern Sichuan and western Guizhou. Under the SSP5-8.5 climate scenario, the area of the moderately suitable areas of *P. yunnanensis* shrink slightly from 2021 to 2040 and the area of the moderately suitable areas is expected to increase in southeastern Tibet, Yunnan, Guizhou, eastern Sichuan and western Guangxi, while the area of highly suitable areas is expected to increase in eastern Sichuan and western Guizhou. From 2061 to 2080, the total area of the suitable growth areas of *P. yunnanensis* will shrink. Compared with 2021 to 2040, the lowly suitable areas will increase by about 53.95 × 10^4 km^2, while the moderately suitable areas will shrink significantly by about 68.29 × 10^4 km^2, and the area of the highly suitable areas will shrink by about 6.43 × 10^4 km^2.

Under the SSP1-2.6 climate scenario, the total area of suitable areas for *T. yunnanensis* is expected to increase from 2021 to 2040, and the area of lowly suitable areas is expected to increase by about 4.79 × 10^4 km^2 in northeastern Sichuan, southwestern Yunnan and northwestern Guizhou. The area of moderately suitable areas is expected to increase by about 9.11 × 10^4 km^2 in northeastern Sichuan, northwestern Guizhou and southeastern Yunnan, and the area of highly suitable areas is expected to increase by about 18.07 × 10^4 km^2 in southeastern Tibet, northeastern Sichuan, western Guizhou and northeastern Yunnan. Compared with 2021–2040, the total area suitable for the growth of *T. yunnanensis* from 2061 to 2080 is expected to be the largest, about 59.47 × 10^4 km^2. Under the SSP5-8.5 climate scenario, from 2021–2040 to 2061–2080, the moderately suitable and highly suitable areas of *T. yunnanensis* are expected to increase substantially and then show a trend of shrinking. It is estimated that the area of the moderately suitable areas from 2061 to 2080 will decrease by 4.08 × 10^4 km^2. Compared with that of 2021 to 2040, the area of the highly suitable areas is expected to decrease by 6.39 × 10^4 km^2.

3.5. Changes in the Potential Distribution of P. yunnanensis and T. yunnanensis

By comparative analysis of suitable areas classes of *P. yunnanensis* and *T. yunnanensis* under different climate scenarios, the spatial variation map of habitat suitability area was mapped (Figure 8). Table 3 shows changes in the potential distribution of *P. yunnanensis* and *T. yunnanensis* under different climate scenarios. Two major observations can be drawn, as shown in Table 3. First, a suitable class 1 area for *P. yunnanensis* is 188.81 × 10^4 km^2, of which 187.78 × 10^4 km^2 is unsuitable for *T. yunnanensis* in the current climate. Under the climatic conditions of SSP1-2.6, the unsuitable areas of *T. yunnanensis* in 2021–2040 and 2061–2080 are 140.78 × 10^4 and 140.61 × 10^4 km^2, respectively, whereas for the years 2021–2040 and 2061–2080 under SSP5-8.5, the areas of unsuitable areas are 141.02 × 10^4 and 160.71 × 10^4 km^2, respectively. Secondly, a suitable class 4 area for *P. yunnanensis* is 5.92 × 10^4 km^2, and the potential distribution for *P. yunnanensis* is the unsuitable area, the lowly suitable area and the moderately suitable area, with an area of 5.6 × 10^4 km^2 in the current climate. Under the SSP1-2.6 climate scenario, a suitable class 4 area for *P. yunnanensis* will shrink by 98.64% and increase by 32.77% in 2021–2040 and 2061–2080 compared with the current climate, respectively, of which the unsuitable area, lowly suitable area and moderately suitable area of *T. yunnanensis* in 2021–2040 will shrink by 45.71% and increase by 6.42% in 2061–2080, respectively. A suitable class 4 area for *P. yunnanensis* will increase by 40.03% and shrink by 68.58% in 2021–2040 and 2061–2080 compared with the current climate, respectively, of which the unsuitable area, lowly suitable area and moderately suitable area of *T. yunnanensis* in 2021–2040 will increase by 215.71% and in 2061–2080 will shrink by 74.11% under the SSP5-8.5 climate scenario, respectively.

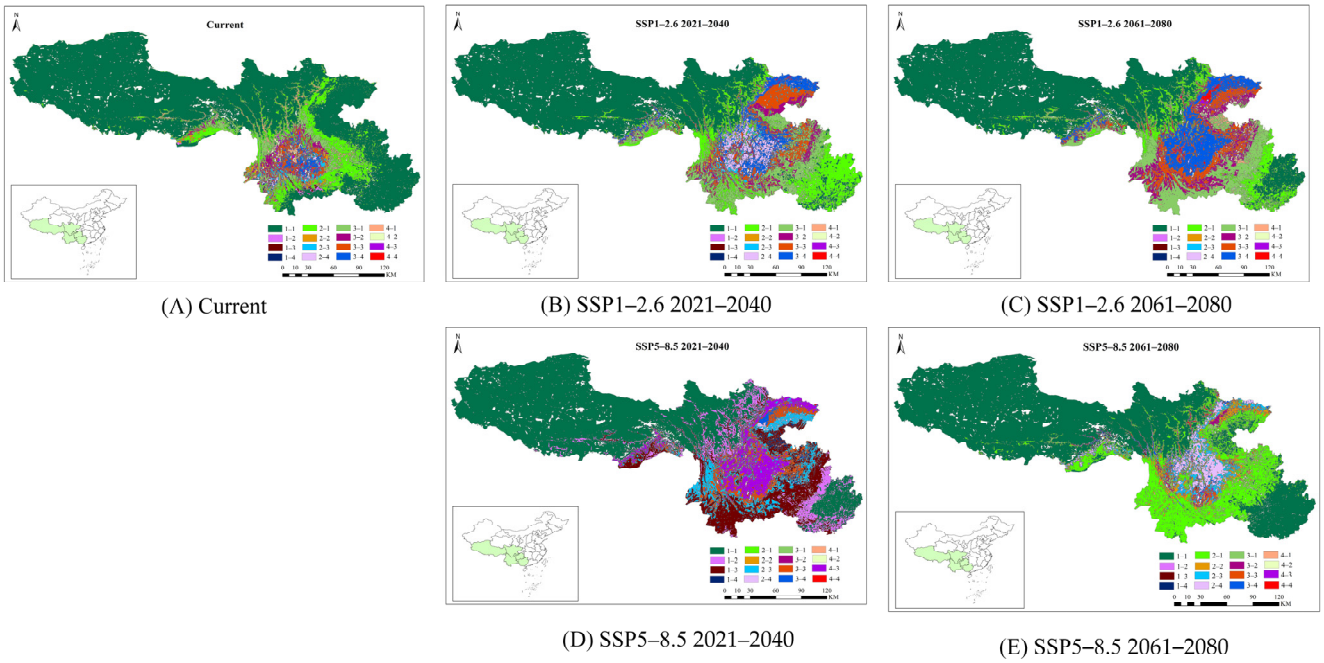

(Λ) Current (B) SSP1–2.6 2021–2040 (C) SSP1–2.6 2061–2080

(D) SSP5–8.5 2021–2040 (E) SSP5–8.5 2061–2080

Figure 8. Changes in the potential distribution of *P. yunnanensis* and *T. yunnanensis* under different climate scenarios. ("1" indicates unsuitable areas, "2" indicates lowly suitable areas, "3" indicates moderately suitable areas, and "4" indicates highly suitable areas).

Table 3. Changes in the potential distribution of *P. yunnanensis* and *T. yunnanensis* under different climate scenarios.

Current		SSP1-2.6				SSP5-8.5			
		2021–2040		2061–2080		2021–2040		2061–2080	
Change	Aera ($\times 10^4$ km^2)	Change	Aera ($\times 10^4$ km^2)	Change	Aera ($\times 10^4$ km^2)	Change	Aera ($\times 10^4$ km^2)	Change	Aera ($\times 10^4$ km^2)
1–1	187.78	1–1	140.78	1–1	140.61	1–1	141.02	1–1	160.71
3–2	4.33	3–2	10.65	3–2	14.68	3–2	0.30	3–2	2.20
3–3	4.76	3–3	14.08	3–3	16.56	3–3	13.32	3–3	2.24
3–4	2.93	3–4	13.92	3–4	21.25	3–4	2.13	3–4	1.70
4–1	2.85	4–1	0.00	4–1	2.12	4–1	0.0	4–1	0.64
4–2	1.37	4–2	0.01	4–2	1.79	4–2	0.21	4–2	0.36
4–3	1.38	4–3	0.03	4–3	2.05	4–3	17.47	4–3	0.45

4. Discussion

4.1. Potential Current Distribution of Suitable Areas for P. yunnanensis and T. yunnanensis

The response curves showed how the predicted probability of presence changed as each environmental variable varied (Figure S1). A probability value greater than MaxSS indicated that the environment was suitable for the growth of *P. yunnanensis* and *T. yunnanensis*. Under current climatic conditions, the area of the currently suitable areas for *P. yunnanensis* is predicted to increase, with a highly suitable altitude of 1500 to 2500 m, an isotherm of 47–49 and a minimum temperature of 2–8 °C in the coldest months. Temperature changes have important effects on plant growth, and at high altitudes, where temperatures are relatively low, the physiological activity of trees is affected; temperature has a strong influence on the length of the growing season, and lower temperatures at high altitudes may shorten the length of the growing season for which plants are suitable [44]. Previous studies [44] have shown that the altitude of the *P. yunnanensis* distribution area is 1000–4000 m, with a larger distribution area at 2000–2500 m above sea level. The results of this study are also similar to those of previous studies.

Temperature and precipitation are the main factors limiting the current distribution of *T. yunnanensis*. The experimental results of the Jackknife method show that the mini-

mum temperature of the coldest month (BIO6) has the greatest influence on the potential distribution of *T. yunnanensis*. Under current climatic conditions, the predicted minimum temperature of the coldest month for *T. yunnanensis* is 0–1 °C (Figure S2). The complex relationship between temperature and physiological processes affects the geographical distribution of species [45]. Since *T. yunnanensis* has almost no overwintering habit, it is a frequent tree resident throughout the year. *T. yunnanensis* also has a long period of adult moth damage and is highly susceptible to multiple tip changes. Typically, in years with moderate precipitation, trees grow extremely well and are highly resistant to insects. Abundant precipitation can curb the insect's multiple translocations to the tops and trunks of trees. In the event of drought or relatively low temperatures, *P. yunnanensis* grows poorly and is poorly resistant to insects; the level of naturally secreted insect-resistant substances in the tree decreases and the release of volatile secretions that attract *T. yunnanensis* to settle increases, thus creating conditions for the reproduction and development of *T. yunnanensis* [46].

4.2. Potential Future Distribution and Relationship between P. yunnanensis and T. yunnanensis

Most previous studies have suggested that climate warming is causing plant and animal species to migrate to higher altitudes and toward polar regions [47–50]. In this study, different climate scenarios are used to predict the potential range changes of *P. yunnanensis* and *T. yunnanensis* (Figures 5–7). The experimental results indicate that under future climate scenarios, the suitable areas of both *P. yunnanensis* and *T. yunnanensis* tend to move to higher altitudes in the west and higher latitudes in the north in response to global climate change. In general, the total area of suitable areas of *P. yunnanensis* increased. This trend is mainly reflected in the increase in the area of low and moderately suitable areas. The increase in the area of the low and moderately suitable areas is mainly manifested in two ways. First, global warming has transformed some areas of the Yunnan-Guizhou–Sichuan Plateau and the Qinghai–Tibet Plateau from initially unsuitable areas to lowly suitable areas and lowly suitable areas to moderately suitable areas [51,52]. Second, under the influence of climate change, some moderate and highly suitable areas are transformed into lowly suitable or even unsuitable areas. This phenomenon suggests that climate change limits the growth of plants in fitness areas, while global warming may also affect plant life activities through photosynthesis and respiration [5]. At the same time, land-use changes caused by human activities, such as changes in management practices and land use, lead to habitat fragmentation [8,9].

Under the future climate scenario of this study, the total suitable area of *T. yunnanensis* is expected to increase in the near future, especially in southeastern Tibet, northeastern Sichuan, western Guizhou and northeastern Yunnan, which may become the distribution centers of this species. Although the magnitude of area change in suitable areas varies under various scenarios, these scenarios will pose serious challenges for *T. yunnanensis* control in the coming decades. Figure 7 shows a clear bottleneck of expansion of *T. yunnanensis* into northeastern Sichuan near the Daba Mountains [53]. Therefore, in the coming decades, we need to focus on strengthening the monitoring and control of *T. yunnanensis* near the Daba Mountains while combining with MaxEnt models to predict the potential distribution of *T. yunnanensis*. At the same time, regular surveys should be conducted to ensure early detection of pest outbreaks, and a sound forest monitoring and reporting system should be established to ensure timely monitoring of climate change impacts on *P. yunnanensis* and *T. yunnanensis*, then timely formulation of *T. yunnanensis* control measures.

In this study, it can be observed from the current and future potential distribution of *P. yunnanensis* and *T. yunnanensis* (Figures 6 and 7, Tables 2 and 3) that under the SSP1-2.6 climate scenario, with the future climate change, the area of suitable habitats for *P. yunnanensis* and *T. yunnanensis* showed an upward trend. Especially in the moderately suitable areas of *P. yunnanensis*, the area of the suitable area for *T. yunnanensis* increased continuously and reached the maximum in 2061–2080. Under the SSP1-2.6 climate scenario, with the passage of time, the highly suitable area of *P. yunnanensis*, the unsuitable area, the lowly suitable area and the moderately suitable area of *T. yunnanensis* have significant

upward trends. This may be related to the combination of socioeconomic trends and climate policies in the SSP1-2.6 scenario leading to an increase in forest area and good growth of *P. yunnanensis* [54]. In contrast, under the SSP5-8.5 climate scenario, in 2061–2080, due to the increase in greenhouse gas emissions and increased climate extremes [55,56], most of the suitable areas of *P. yunnanensis* change from moderately and highly suitable areas to lowly suitable areas due to poor growth and insect resistance of *P. yunnanensis* (Figure 6), resulting in the proliferation of *T. yunnanensis*. Therefore, under the SSP5-8.5 climate scenario, with the future climate change, the suitable areas of *P. yunnanensis* and *T. yunnanensis* showed a trend of first increasing and then decreasing (the highest in 2021–2040).

5. Conclusions

This study predicted the potential distribution of *P. yunnanensis* and *T. yunnanensis* under two periods and two shared socioeconomic pathways using the MaxEnt model. Under current climatic conditions, elevation (ELEV), the minimum temperature in the coldest month (BIO6) and annual temperature range (BIO7) constrain the current distribution of *P. yunnanensi*. The minimum temperature in the coldest month (BIO6), elevation (ELEV) and minimum temperature in the coldest month (BIO6) are the most important variable of the current distribution of *T. yunnanensis*. Under different climate change scenarios, the adaptation areas of *P. yunnanensis* and *T. yunnanensis* are increasing, and both have a tendency to move to higher altitudes in the west and higher latitudes in the north. At the same time, this study found an obvious bottleneck of expansion to the northeast of Sichuan near the Daba Mountains, which provides a possible solution for controlling *T. yunnanensis*. This study provides an important basis for the breeding of *P. yunnanensis* and controlling *T. yunnanensis*. However, this study only considers the influence of climatic factors in the woldclime database. In future research, the impact of human activities and economic development on *P. yunnanensis* and *T. yunnanensis* will be further studied.

Supplementary Materials: The following supporting information can be downloaded at: https://www.mdpi.com/article/10.3390/f13091379/s1, Figure S1: Response curves of 10 environmental variables in a potential distribution model of *P. yunnanensis*; Figure S2: Response curves of 10 environmental variables in a potential distribution model of *T. yunnanensis*.

Author Contributions: Conceptualization, B.H. and J.M.; methodology, B.H. and Y.C.; software, B.H. and Y.S.; validation, B.H., Y.Z. and J.M.; investigation, B.H. and Y.S.; data curation, J.M. and Y.C.; writing—original draft preparation, B.H.; writing—review and editing, Y.Z., Y.S. and Y.C.; supervision, Y.Z. and Z.X.; project administration, Y.Z.; funding acquisition, Y.Z. All authors have read and agreed to the published version of the manuscript.

Funding: This work was supported by projects of National Natural Science Foundation to Y.Z.; Digitalization, development and application of biotic resource; Key Laboratory for Forest Resources Conservation to Z.X. and Utilization in the Southwest Mountains of China, Ministry of Education to Y.Z., grant numbers 31960142, 202002AA10007 and KLESWFU-201905, respectively.

Institutional Review Board Statement: Not applicable.

Informed Consent Statement: Not applicable.

Data Availability Statement: Not applicable.

Conflicts of Interest: The authors declare no conflict of interest.

References

1. IPCC. Summary for Policymakers. In *Climate Change 2021: The Physical Science Basis. Contribution of Working Group I to the SixthAssessment Report of the Intergovernmental Panel on Climate Change*; Intergovernmental Panel on Climate Change: Cambridge, UK; New York, NY, USA, 2021.
2. Ying, Z. Projections of 2.0 °C Warming over the Globe and China under RCP4.5. *Atmos. Ocean. Sci. Lett.* **2012**, *5*, 514–520. [CrossRef]
3. Zhao, D.S.; Gao, X.; Wu, S.G.; Zheng, D. Trend of climate variation in China from 1960 to 2018 based on natural regionalization. *Adv. Earth Sci.* **2020**, *35*, 750–760.

4. Guo, Y.; Li, X.; Zhao, Z.; Nawaz, Z. Predicting the impacts of climate change, soils and vegetation types on the geographic distribution of Polyporus umbellatus in China. *Sci. Total Environ.* **2019**, *648*, 1–11. [CrossRef] [PubMed]
5. Wang, X.; Zhang, W.; Zhao, X.; Zhu, H.; Ma, L.; Qian, Z.; Zhang, Z. Modeling the Potential Distribution of Three Taxa of Akebia Decne. Under Climate Change Scenarios in China. *Forests* **2021**, *12*, 1710.
6. Dawson, T.P.; Jackson, S.T.; House, J.I.; Prentice, I.C.; Mace, G.M. Beyond Predictions: Biodiversity Conservation in a Changing Climate. *Science* **2011**, *332*, 53–58. [CrossRef]
7. Yin, Y.; He, Q.; Pan, X.; Liu, Q.; Wu, Y.; Li, X. Predicting Current Potential Distribution and the Range Dynamics of Pomacea canaliculata in China under Global Climate Change. *Biology* **2022**, *11*, 110. [CrossRef]
8. Chen, Y.G.; Yue, X.G.; Chen, Y.H.; Cheng, W.X.; Du, G.J.; Zhong, Q.L.; Cheng, Q.L. Identification of potential distribution area of Cunninghamia lanceolata in China under climate change based on the MaxEnt model. *Chin. J. Appl. Ecol.* **2022**, *33*, 1207–1214.
9. Haddad, N.M.; Brudvig, L.A.; Clobert, J.; Davies, K.F.; Gonzalez, A.; Holt, R.D.; Lovejoy, T.E.; Sexton, J.O.; Austin, M.P.; Collins, C.D.; et al. Habitat fragmentation and its lasting impact on Earth's ecosystems. *Sci. Adv.* **2015**, *1*, e1500052. [CrossRef]
10. Bálint, M.; Domisch, S.; Engelhardt, C.H.M.; Haase, P.; Lehrian, S.; Sauer, J.; Theissinger, K.; Pauls, S.U.; Nowak, C. Cryptic biodiversity loss linked to global climate change. *Nat. Clim. Chang.* **2011**, *1*, 313–318. [CrossRef]
11. Oliver, T.; Hill, J.K.; Thomas, C.D.; Brereton, T.; Roy, D.B. Changes in habitat specificity of species at their climatic range boundaries. *Ecol. Lett.* **2009**, *12*, 1091–1102. [CrossRef]
12. Peterson, M.L.; Doak, D.F.; Morris, W.F. Incorporating local adaptation into forecasts of species' distribution and abundance under climate change. *Glob. Chang. Biol.* **2019**, *25*, 775–793. [PubMed]
13. Anderson, R.P. A framework for using niche models to estimate impacts of climate change on species distributions. *Ann. N. Y. Acad. Sci.* **2013**, *1297*, 8–28. [CrossRef] [PubMed]
14. Elith, J.; Leathwick, J.R. Species Distribution Models: Ecological Explanation and Prediction Across Space and Time. *Annu. Rev. Ecol. Evol. Syst.* **2009**, *40*, 677–697. [CrossRef]
15. Qiao, H.J.; Hu, J.H.; Huang, J.H. Theoretical basis, future directions, and challenges for ecological niche models. *Sci. Sin.* **2013**, *43*, 915–927. [CrossRef]
16. Li, Y.; Li, M.; Li, C.; Liu, Z. Optimized Maxent Model Predictions of Climate Change Impacts on the Suitable Distribution of Cunninghamia lanceolata in China. *Forests* **2020**, *11*, 302. [CrossRef]
17. Dang, A.T.N.; Kumar, L.; Reid, M. Modelling the Potential Impacts of Climate Change on Rice Cultivation in Mekong Delta, Vietnam. *Sustainability* **2020**, *12*, 9608. [CrossRef]
18. Kogo, B.K.; Kumar, L.; Koech, R.; Kariyawasam, C.S. Modelling Climate Suitability for Rainfed Maize Cultivation in Kenya Using a Maximum Entropy (MaxENT) Approach. *Agronomy* **2019**, *9*, 727. [CrossRef]
19. Li, H.Q.; Liu, X.H.; Wang, J.H.; Xing, L.G.; Fu, Y.Y. Maxent modelling for predicting climate change effects on the potential planting area of tuber mustard in China. *J. Agric. Sci.* **2019**, *157*, 375–381. [CrossRef]
20. Ma, Y.; Lu, X.; Li, K.; Wang, C.; Guna, A.; Zhang, J. Prediction of Potential Geographical Distribution Patterns of Actinidia arguta under Different Climate Scenarios. *Sustainability* **2021**, *13*, 3526. [CrossRef]
21. Çoban, H.O.; Örücü, Ö.K.; Arslan, E.S. MaxEnt Modeling for Predicting the Current and Future Potential Geographical Distribution of Quercus libani Olivier. *Sustainability* **2020**, *12*, 2671. [CrossRef]
22. Zhao, H.; Zhang, H.; Xu, C. Study on Taiwania cryptomerioides under climate change: MaxEnt modeling for predicting the potential geographical distribution. *Glob. Ecol. Conserv.* **2020**, *24*, e01313. [CrossRef]
23. Koo, K.S.; Park, D.; Oh, H.S. Analyzing habitat characteristics and predicting present and future suitable habitats of Sibynophis chinensis based on a climate change scenario. *J. Asia-Pac. Biodivers.* **2019**, *12*, 1–6. [CrossRef]
24. Saeedi, H.; Costello, M.J.; Warren, D.; Brandt, A. Latitudinal and bathymetrical species richness patterns in the NW Pacific and adjacent Arctic Ocean. *Sci. Rep.* **2019**, *9*, 9303. [CrossRef]
25. Saeedi, H.; Basher, Z.; Costello, M.J. Modelling present and future global distributions of razor clams (Bivalvia: Solenidae). *Helgol. Mar. Res.* **2016**, *70*, 235. [CrossRef]
26. Jones, M.C.; Dye, S.R.; Pinnegar, J.K.; Warren, R.; Cheung, W.W.L. Modelling commercial fish distributions: Prediction and assessment using different approaches. *Ecol. Model.* **2012**, *225*, 133–145. [CrossRef]
27. Yi, Y.-j.; Cheng, X.; Yang, Z.-F.; Zhang, S.-H. Maxent modeling for predicting the potential distribution of endangered medicinal plant (*H. riparia* Lour) in Yunnan, China. *Ecol. Eng.* **2016**, *92*, 260–269. [CrossRef]
28. Du, Z.; He, Y.; Wang, H.; Wang, C.; Duan, Y. Potential geographical distribution and habitat shift of the genus Ammopiptanthus in China under current and future climate change based on the MaxEnt model. *J. Arid. Environ.* **2021**, *184*, 104328. [CrossRef]
29. Anand, V.; Oinam, B.; Singh, I.H. Predicting the current and future potential spatial distribution of endangered Rucervus eldii eldii (Sangai) using MaxEnt model. *Environ. Monit. Assess.* **2021**, *193*, 147. [CrossRef]
30. Thapa, A.; Wu, R.; Hu, Y.; Nie, Y.; Singh, P.B.; Khatiwada, J.R.; Yan, L.; Gu, X.; Wei, F. Predicting the potential distribution of the endangered red panda across its entire range using MaxEnt modeling. *Ecol. Evol.* **2018**, *8*, 10542–10554. [CrossRef]
31. Ning, H.; Tang, M.; Chen, H. Impact of Climate Change on Potential Distribution of Chinese White Pine Beetle Dendroctonus armandi in China. *Forests* **2021**, *12*, 544. [CrossRef]
32. Negrini, M.; Fidelis, E.G.; Picanco, M.C.; Ramos, R.S. Mapping of the Steneotarsonemus spinki invasion risk in suitable areas for rice (*Oryza sativa*) cultivation using MaxEnt. *Exp. Appl. Acarol.* **2020**, *80*, 445–461. [CrossRef] [PubMed]

33. Zhu, H.; Kumar, S.; Neven, L.G. Codling Moth (Lepidoptera: Tortricidae) Establishment in China: Stages of Invasion and Potential Future Distribution. *J. Insect. Sci.* **2017**, *17*, 85. [CrossRef] [PubMed]
34. Wang, R.; Yang, H.; Luo, W.; Wang, M.; Lu, X.; Huang, T.; Zhao, J.; Li, Q. Predicting the potential distribution of the Asian citrus psyllid, *Diaphorina citri* (Kuwayama), in China using the MaxEnt model. *PeerJ* **2019**, *7*, e7323. [CrossRef] [PubMed]
35. Huang, B.; Liu, J.; Jiao, J.; Lu, J.; Lv, D.; Mao, J.; Zhao, Y.; Zhang, Y. Applications of machine learning in pine nuts classification. *Sci. Rep.* **2022**, *12*, 8799. [CrossRef]
36. Chen, J.; Zhang, S.S.; Luo, T.; Zheng, W.; Yang, W.Z.; Li, J.W.; Wang, Y.B.; Wang, S. Distribution patterns of *Pinus yunnanensis* and *P. yunnanensis* var.pygmaea and related key ecological factors. *J. Northeast. For. Univ.* **2021**, *49*, 8–14.
37. Wang, X.W.; Chen, P.; Wang, Y.X.; Yuan, R.L.; Feng, D.; Li, L.S.; Ye, H.; Pan, Y.; Lv, J.; Zhou, Y.F.; et al. Population Structure and Succession Law of Tomicus Species in Yunnan. *For. Res.* **2018**, *31*, 167–172.
38. Yan, G.; Zhang, M.D.; Qian, L.B.; Ze, S.X.; Yang, B.; Li, Z.B. Electrophysiological and behavioral responses of Tominus yunnanensis to plant volatiles from primarily infected pinus yunnanensis in Yunnan, Southwest China. *J. Environ. Entomol.* **2021**, *43*, 1389–1397.
39. Wu, T.; Lu, Y.; Fang, Y.; Xin, X.; Liu, X. The Beijing Climate Center Climate System Model (BCC-CSM): Main Progress from CMIP5 to CMIP6. *Geosci. Model Dev. Discuss.* **2019**, *12*, 1573–1600. [CrossRef]
40. Xu, W.; Xiao, Y.; Zhang, J.; Yang, W.; Zhang, L.; Hull, V.; Wang, Z.; Zheng, H.; Liu, J.; Polasky, S.; et al. Strengthening protected areas for biodiversity and ecosystem services in China. *Proc. Natl. Acad. Sci. USA* **2017**, *114*, 1601–1606. [CrossRef]
41. Alcala-Canto, Y.; Alberti-Navarro, A.; Figueroa-Castillo, J.A.; Ibarra-Velarde, F.; Vera-Montenegro, Y.; Cervantes-Valencia, M.E. Maximum Entropy Ecological Niche Prediction of the Current Potential Geographical Distribution of Eimeria Species of Cattle, Sheep and Goats in Mexico. *Open J. Anim. Sci.* **2019**, *09*, 234–248. [CrossRef]
42. Zhao, Y.; Zhao, M.; Zhang, L.; Wang, C.; Xu, Y. Predicting Possible Distribution of Tea (*Camellia sinensis* L.) under Climate Change Scenarios Using MaxEnt Model in China. *Agriculture* **2021**, *11*, 1122. [CrossRef]
43. Gebrewahid, Y.; Abrehe, S.; Meresa, E.; Eyasu, G.; Abay, K.; Gebreab, G.; Kidanemariam, K.; Adissu, G.; Abreha, G.; Darcha, G. Current and future predicting potential areas of *Oxytenanthera abyssinica* (A. Richard) using MaxEnt model under climate change in Northern Ethiopia. *Ecol. Processes* **2020**, *9*, 6. [CrossRef]
44. Swets, J. Measuring the accuracy of diagnostic systems. *Science* **1988**, *240*, 1285–1293. [CrossRef] [PubMed]
45. Lu, S.F.; Chen, Y.H.; Zhou, S.Y.; Yin, X.J. Responses of Pinus species to climate change in southwestern China. *J. For. Environ.* **2020**, *40*, 466–477.
46. Yang, R.Q.; Fan, Z.X.; Li, Z.S.; Wen, Q.Z. Radial growth of *Pinus yunnanensis* at different elevations and their responses to climatic factors in the Yulong Snow Mountain, Northwest Yunnan, China. *Acta Ecol. Sin.* **2018**, *38*, 8983–8991.
47. Regniere, J.; Powell, J.; Bentz, B.; Nealis, V. Effects of temperature on development, survival and reproduction of insects: Experimental design, data analysis and modeling. *J. Insect Physiol.* **2012**, *58*, 634–647. [CrossRef]
48. Wang, Q. Effect of Extreme Climate on the Occurrence Tendency of Three Forest Pests. Master's Thesis, Chinese Academy of Forestry, Beijing, China, July 2016.
49. Chen, I.C.; Hill, J.K.; Ohlemuller, R.; Roy, D.B.; Thomas, C.D. Rapid range shifts of species associated with high levels of climate warming. *Science* **2011**, *333*, 1024–1026. [CrossRef]
50. Thomas, C.D.; Gillingham, P.K. The performance of protected areas for biodiversity under climate change. *Biol. J. Linn. Soc.* **2015**, *115*, 718–730. [CrossRef]
51. Rew, L.J.; McDougall, K.L.; Alexander, J.M.; Daehler, C.C.; Essl, F.; Haider, S.; Kueffer, C.; Lenoir, J.; Milbau, A.; Nuñez, M.A.; et al. Moving up and over: Redistribution of plants in alpine, Arctic, and Antarctic ecosystems under global change. *Arct. Antarct. Alp. Res.* **2020**, *52*, 651–665. [CrossRef]
52. Hu, R.; Gu, Y.; Luo, M.; Lu, Z.; Wei, M.; Zhong, J. Shifts in bird ranges and conservation priorities in China under climate change. *PLoS ONE* **2020**, *15*, e0240225. [CrossRef]
53. Weber, T.C. Maximum entropy modeling of mature hardwood forest distribution in four U.S. states. *For. Ecol. Manag.* **2011**, *261*, 779–788. [CrossRef]
54. Chen, Y.H.; Lv, Y.W.; Yin, X.J. Predicting habitat suitability of 12 coniferous forest tree species in southwest China based on climate change. *J. Nanjing For. Univ. (Nat. Sci. Ed.).* **2019**, *43*, 113–120.
55. Li, X.; Ma, B.; Lu, C.; Yang, H.; Sun, M. Spatial Pattern and Development of Protected Areas in the North-south Transitional Zone of China. *Chin. Geogr. Sci.* **2021**, *31*, 149–166. [CrossRef]
56. Hurtt, G.C.; Chini, L.; Sahajpal, R.; Frolking, S.; Bodirsky, B.L.; Calvin, K.; Doelman, J.C.; Fisk, J.; Fujimori, S.; Klein Goldewijk, K.; et al. Harmonization of global land use change and management for the period 850–2100 (LUH2) for CMIP6. *Geosci. Model Dev.* **2020**, *13*, 5425–5464. [CrossRef]